Materials Today Physics 6 (2018) 83–88

Contents lists available at ScienceDirect

Materials Today Physics

journal homepage: https://www.journals.elsevier.com/materials-today-physics

Heat capacity of Mg_3Sb_2, Mg_3Bi_2, and their alloys at high temperature

Matthias T. Agne [a, *], Kazuki Imasato [a], Shashwat Anand [a], Kathleen Lee [b], Sabah K. Bux [b], Alex Zevalkink [c], Alexander J.E. Rettie [d], Duck Young Chung [d], Mercouri G. Kanatzidis [d, e], G. Jeffrey Snyder [a, **]

[a] Dept. Materials Science and Engineering, Northwestern University, Evanston, IL 60208, USA
[b] Thermal Energy Conversion Research and Advancement Group, Jet Propulsion Laboratory/California Institute of Technology, Pasadena, CA 91109, USA
[c] Dept. Materials Science and Engineering, Michigan State University, East Lansing, MI 48824, USA
[d] Materials Science Division, Argonne National Laboratory, Argonne, IL 60439, USA
[e] Dept. Chemistry, Northwestern University, Evanston, IL 60208, USA

ARTICLE INFO

Article history:
Received 13 September 2018
Received in revised form
26 September 2018
Accepted 1 October 2018
Available online 3 November 2018

Keywords:
Thermoelectric
Mg_3Sb_2
Mg_3Bi_2
Heat capacity
Thermal conductivity

ABSTRACT

The thermoelectric figure of merit reported for n-type $Mg_3(Sb,Bi)_2$ compounds has made these materials of great engineering significance, increasing the need for accurate evaluations of their thermal conductivity. Thermal conductivity is typically derived from measurements of thermal diffusivity and determination of the specific heat capacity. The uncertainty in this method (often 10% or more) is frequently attributed to measurement of heat capacity such that estimated values are often more accurate. Inconsistencies between reported thermal conductivity of $Mg_3(Sb,Bi)_2$ compounds may be attributed to the different values of heat capacity measured or used to calculate thermal conductivity. The high anharmonicity of these materials can lead to significant deviations at high temperatures from the Dulong-Petit heat capacity, which is often a reasonable substitute for measurements at high temperatures. Herein, a physics-based model is used to assess the magnitude of the heat capacity over the entire temperature range up to 800 K. The model agrees in magnitude with experimental low-temperature values and reproduces the linear slope observed in high-temperature data. Owing to the large scatter in experimental values of high-temperature heat capacity, the model is likely more accurate (within ±3%) than a measurement of a new sample even for doped or alloyed materials. It is found that heat capacity for the solid solution series can be simply described (for temperatures: 200 K ≤ T ≤ 800 K) by the polynomial equation:

$$c_p\left[\mathrm{Jg^{-1}K^{-1}}\right] = \frac{3NR}{M_W}\left(1 + 1.3\times10^{-4}\,T - 4\times10^{3}\,T^{-2}\right),$$

where $3NR = 124.71\ \mathrm{J\,mol^{-1}K^{-1}}$, M_W is the molecular weight [g mol^{-1}] of the formula unit being considered, and T is temperature in K. This heat capacity is recommended to be a standard value for reporting and comparing the thermal conductivity of $Mg_3(Sb,Bi)_2$ including doped or alloyed derivatives. A general form of the equation is given which can be used for other material systems.

1. Introduction

The high thermoelectric performance reported for n-type $Mg_3(Sb,Bi)_2$ compounds has attracted much interest and has initiated a great effort to optimize this material [1–13]. One of the origins of this high performance in the $Mg_3(Sb,Bi)_2$ system is its anomalously low thermal conductivity, which is attributed to the undersized Mg cation and the corresponding soft, anharmonic Mg–Sb bonds [6,14]. Because of the high thermoelectric performance, this material possesses a large potential to be used for practical thermoelectric applications, such as power generation for space probes, etc.

* Corresponding author.
** Corresponding author.
E-mail addresses: mt.agne.matsci@gmail.com (M.T. Agne), jeff.snyder@northwestern.edu (G.J. Snyder).

https://doi.org/10.1016/j.mtphys.2018.10.001
2542-5293/

However, the heat capacity values of $Mg_3(Sb,Bi)_2$, which are required to calculate thermal conductivity, are inconsistent between studies [1,15–17]. At high temperature, the deviation of heat capacity data is more than 10% among previous reports. Before thermoelectric applications can be considered, it is vital to obtain reliable and consistent thermal conductivity data in this system. Temperature-dependent heat capacity data are required to calculate thermal conductivity, κ, through the relation:

$$\kappa = \rho c_p D, \tag{1}$$

where $D[m^2s^{-1}]$ is the thermal diffusivity and $C_p = \rho c_p$ is the volumetric heat capacity $[J\,m^{-3}K^{-1}]$, typically calculated from experimental bulk density, ρ [kg m^{-3}], and the mass specific heat, c_p[J $kg^{-1}K^{-1}$]. Although the various reports rely on the laser flash method to measure D, different reports have used different values of C_p. These different values of heat capacity directly correspond to an overestimation/underestimation of the thermoelectric figure of merit, zT, and leads to a loss of consistency among data reported from different groups.

The problem with experimentally obtained C_p lies in the uncertainty of the heat capacity measurement at high temperature due to the difficulty of the calibration and temperature control [18,19]. Because of this uncertainty, it is often more accurate to use the Dulong-Petit value of heat capacity which is temperature independent. The Dulong–Petit value is often discussed as a specific heat at constant volume C_v because it not only contains contributions to the specific heat from anharmonic effects [20] (e.g. thermal expansion) but also ignores the heat capacity due to electronic carriers, formation of vacancies, etc. Near room temperature, these effects are typically smaller than 5% of the Dulong–Petit value. At higher temperatures, however, these temperature-dependent contributions to C_p can become appreciable, such that estimates of zT can be affected by 10–20%. For example, a ≈15% difference in zT at 725 K was obtained for an $Mg_3(Sb,Bi)_2$ alloy depending on if the Dulong–Petit or an experimental heat capacity was used (compare zT in Refs. [3,4]). Thus, for systems such as $Mg_3(Sb,Bi)_2$ where 10% accuracy in thermal conductivity (and zT) is desired, it is imperative to obtain reliable heat capacity values for precise evaluation of the thermoelectric performance, as has been done for PbTe [21].

In this study, we successfully establish a physics-based model to evaluate C_p at high temperature by considering the contribution from thermal expansion combined with experimentally measured low-temperature heat capacity. It is found that the high-temperature heat capacity of the entire solid solution range can be simply described by a single polynomial equation that should be a new standard for calculating the thermal conductivity of $Mg_3(Sb,Bi)_2$.

2. Methods

Single-phase n-type compositions of $Mg_{3+\delta}(Sb_{2-x}Bi_x)_{1.99}Te_{0.01}$ (x = 0, 0.5, 1.0, 1.5, 2.0) were prepared by methods described elsewhere [5]. In short, elemental Mg (turnings, 99.98%, Alfa Aesar, 99.9%, Alfa Aesar), Sb (shots, 99.9999%, Alfa Aesar, 99.9%, Alfa Aesar), Bi (granules, 99.997%, Alfa Aesar, 99.9%, Alfa Aesar), and Te (lumps, 99.999%, Alfa Aesar) were mixed in the appropriate stoichiometric ratio, sealed in a stainless steel vial under argon atmosphere, and high energy ball milling for 2 h followed by hot pressing at 873 K and 45 MPa for 1 h. The resulting pellets had a bulk density >94% of the theoretical value.

Low-temperature heat capacity was measured from 1.8 to 220 K using a Quantum Design Dynacool physical properties measurement system. Apiezon N grease was used to couple samples to the heat capacity option stage. A semi-adiabatic thermal relaxation method as used, and data were collected on warming. A Netzsch 404 F3 Pegasus differential scanning calorimeter was used to measure the $Mg_3(Sb,Bi)_2$ samples from 375 to 750 K at a heating/cooling rate of 10 K/min in Ar atmosphere. High-temperature heat capacity was calculated by the ratio method using a sapphire standard. The baseline signal of the aluminum crucible, measured under the same conditions, was subtracted from both the sapphire and sample measurements.

The linear thermal expansion coefficient of polycrystalline samples was measured by dilatometry. The sample length was measured as a function of temperature from 300 to 773 K at a heating/cooling rate of 10 K/min in He atmosphere using a Netzsch DIL 402c dilatometer with an alumina pushrod. In the isotropic approximation for polycrystalline materials, the volumetric thermal expansion coefficient is three times the linear thermal expansion coefficient (i.e. $\alpha_V \cong 3 \times 22.3 \times 10^{-6}K^{-1}$).

Longitudinal and transverse speeds of sound [m s^{-1}] (v_L and v_T, respectively) were characterized by pulse-echo ultrasound, using a 5-MHz transducer in a manner previously described [22]. The bulk modulus was calculated as $B = \rho\left(v_L^2 - \frac{4}{3}v_T^2\right)$, the shear modulus was calculated as $G = \rho v_T^2$, and the Debye temperature was calculated as $\theta_D = (\hbar/k_B)(6\pi^2 n)^{1/3} v_s$, where $v_s = \left[\frac{1}{3}\left(\frac{2}{v_T^3} + \frac{1}{v_L^3}\right)\right]^{-\frac{1}{3}}$ is an average speed of sound and n is the number density of atoms [23].

The density functional theory (DFT) calculations [24] in this study were performed using Vienna ab initio simulation package (VASP) [25]. We have used Perdew–Burke–Ernzerhof (PBE) formulation of the exchange–correlation energy functional derived under a gradient-generalized approximation (GGA) [26]. Plane-wave basis sets are truncated at an energy cutoff of 315 eV, and a Gamma-centered k-point mesh with a density of ~8000 k-points per reciprocal atom (KPPRA) was used. The phonon density of states were calculated by performing frozen phonon calculation implemented in the phonopy package [27]. The isotropic speeds of sound were calculated using the Christoffel code [28]. The elastic modulus tensor input for the code was calculated from the density functional perturbation theory (DFPT) capabilities implemented in the VASP code. The Mg_3Bi_2 structure exhibits imaginary frequencies, suggesting a lattice instability at low temperatures (T = 0 K). However, the density of states associated with the unstable modes was small in comparison to all the other modes of the structure combined. As these modes will have a negligible contribution to the heat capacity, the density of states at $\omega = 0$ is set to zero by assuming a Debye-like ω^2 dependence at low frequencies using the calculated isotropic speed of sound.

A physics-based model for the full-range heat capacity at constant pressure C_p was constructed using the thermodynamic relation,

$$C_p = C_v + B\alpha_V^2 T = C_v(1 + \gamma\alpha_V T)\,. \tag{2}$$

Here, the first-order difference between C_p and the heat capacity at constant volume, C_v, is the contribution due to dilation of the material via thermal expansion, where α_V is the volumetric thermal expansion coefficient, B is the isothermal bulk modulus, $\gamma = B\alpha_V/C_v$ is the Gruneisen parameter, and T is the absolute temperature. Additional contributions to C_p from electronic carriers and vacancies were also considered, but not included in the model. For one, no discernible electronic contribution to the heat capacity was observed in low-temperature measurements, as is expected for

carrier concentrations less than 10^{21} cm^{-3}. Furthermore, the contribution from Mg vacancies can be estimated in the dilute limit as $C_{p,vac} \approx R\left(\frac{\Delta H_{vac}}{RT}\right)^2 e^{-\frac{\Delta H_{vac}}{RT}}$, where ΔH_{vac} is the vacancy formation energy ($\approx$53 kJ mol^{-1} for Mg vacancies in degenerate n-type Mg_3Sb_2 material [3]), resulting in $C_{p,vac} < 0.2\%$ of the Dulong–Petit value at 800 K.

When the phonon density of states, $g(\omega)$, can be considered as temperature independent, C_v can be calculated using

$$C_v = 3nk_B \int_0^\infty \left(\frac{g(\omega)}{3n}\right)\left(\frac{\hbar\omega}{k_B T}\right)^2 \left(e^{\frac{\hbar\omega}{k_B T}}\right)\left(e^{\frac{\hbar\omega}{k_B T}} - 1\right)^{-2} d\omega, \quad (3)$$

where n is the number density of atoms, $g(\omega)/3n$ is the normalized density of states ($\int_0^\infty [g(\omega)/3n]d\omega = 1$), k_B is the Boltzmann constant, and $\hbar$ is the reduced Planck constant. This integral was evaluated numerically using a spline fit of the DFT-calculated normalized density of states (Fig. 2B).

Note that to convert the units of Eq. (2) from J m^{-3}K^{-1} to J mol^{-1}K^{-1}, it is necessary to multiply by the molar volume, V_m[m^{3}mol^{-1}], of the compound being considered. This can be accomplished using the relationship between V_m, molecular weight, M_W [kg mol^{-1}], and density, ρ [kg m^{-3}]: $V_m = M_W/\rho$. Implicit in this notation is that the molar quantity, mol, is really moles of formula units.

3. Results and discussion

The Mg_3Sb_2 and Mg_3Bi_2 compounds are known to have soft shear moduli and highly anharmonic bonding compared with other isostructural compounds (e.g. $CaMg_2Sb_2$) [6,29]. These characteristics contribute to the low lattice thermal conductivity that makes $Mg_3Sb_{2-x}Bi_x$ alloys promising for thermoelectric applications. However, the high anharmonicity present in these compounds means that the use of the Dulong–Petit heat capacity is likely a significant underestimate at high temperatures.

This study used low-temperature heat capacity measurements to determine the Debye temperature for a series of $Mg_3Sb_{2-x}Bi_x$ compounds (x = 0, 0.5, 1.0, 1.5, 2). By plotting C_p/T^3 vs T, it is possible to determine the so-called Debye level, β. This horizontal plateau is observed when atomic vibrations dominate the heat capacity in the $T \to 0$ K limit (i.e. $g(\omega) \propto \omega^2$) and is related to the Debye temperature using the relation $\theta_D = \left(\frac{12}{5}\pi^4 NR\right)^{1/3} \beta^{-1/3}$, where β has units of J mol^{-1}K^{-4}, N is the number of atoms per formula unit, and R is the gas constant. In Fig. 1a, the experimental values of C_p/T^3 are plotted along with corresponding Debye model fits of β. The Debye temperatures obtained from pulse-echo speed of sound measurements are in excellent agreement with those determined from heat capacity (Fig. 1b). Clearly, there is an elastic softening as Mg_3Sb_2 is alloyed with Mg_3Bi_2 that appears to follow a linear relation (Vegard's law) with composition. Interestingly, although the Debye temperature decreases by 23%, the bulk modulus remains nearly constant across the compositional range (Table 1). This indicates that it is predominantly the shear modes that soften during alloying.

Thermal expansion is an inherently anharmonic effect, such that more anharmonicity tends to result in larger thermal expansion coefficients. The volumetric thermal expansion coefficient α_V, determined by dilatometry (66.9×10^{-6}K^{-1}), is comparable with that of other anharmonic thermoelectric materials such as PbTe (59.1×10^{-6}K^{-1}) and SnTe (63.9×10^{-6}K^{-1}) [30]. However, temperature-dependent X-ray diffraction results obtained herein gave a 37% lower absolute magnitude of α_V, likely resulting from a systemic error in the temperature control. Nevertheless, the X-ray measurements indicate that the thermal expansion coefficient is independent of composition, within 10%. Previous experimental and computational work on Mg_3Sb_2 reported α_V values of 51.9×10^{-6}K^{-1} and 61.7×10^{-6}K^{-1} at 300 K [6]. These values are larger than those for the isostructural compounds $CaMg_2Sb_2$ and $CaMg_2Bi_2$ (and the Yb analogues), again due to the larger anharmonicity of $Mg_3(Sb,Bi)_2$. Computational values as large as almost 90×10^{-6}K^{-1} were reported for Mg_3Sb_2 at 600 K [6]. However, experimentally, there is no indication of a significant increase in α_V from 300 to 720 K.

Experimental heat capacities of Mg_3Sb_2 and Mg_3Bi_2 from 2 to 220 K can be well described using Eq. (2) (Fig. 2a). The DFT-calculated density of states (Fig. 2b, used in Eq. (3)) also shows that Mg_3Bi_2 is softer than Mg_3Sb_2, in agreement with the trend in Debye temperatures (Fig. 1b). A constant value of $B\alpha_V^2 = 206.9$ J m^{-3}K^{-2} is used based on the average measured value of bulk modulus (46.2 GPa, Table 1) and the high-temperature value for the volumetric thermal expansion coefficient ($66.9 \times$

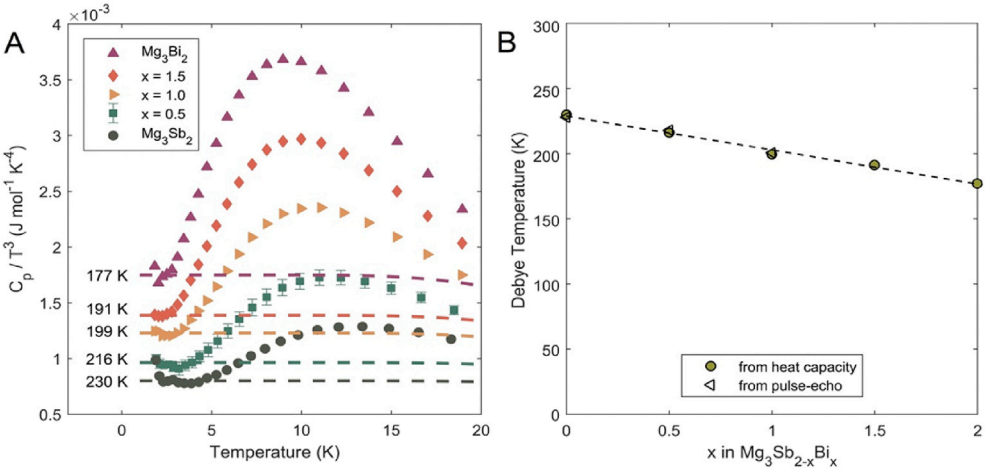

Fig. 1. (**a**) Measured values of molar heat capacities plotted as C_p/T^3 vs T (markers) for several compositions in the $Mg_3Sb_{2-x}Bi_x$ system, with corresponding Debye model curves (dashed lines) and (**b**) the Debye temperatures obtained from the data shown in panel (a) and from pulse-echo speed of sound data, plotted vs nominal composition.

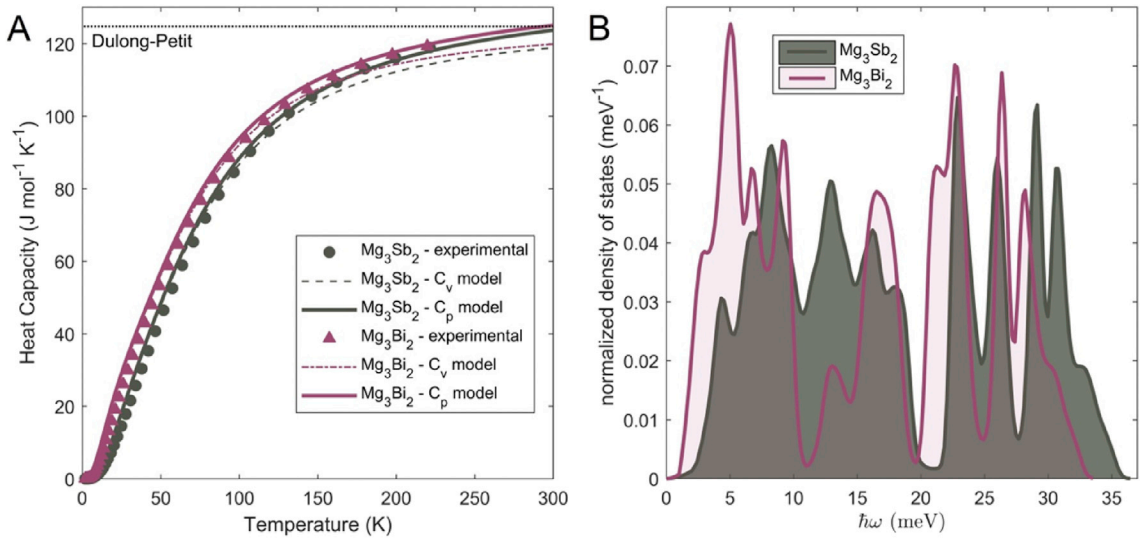

Fig. 2. (**a**) Measurements of low-temperature molar heat capacities of Mg_3Sb_2 (grey circles) and Mg_3Bi_2 (purple triangles) modeled by Eq. (2) (solid lines), using the linear dilation term discussed in text and the constant volume heat capacity (dashed lines) calculated using (**b**) the DFT phonon densities of states of Mg_3Sb_2 (grey shaded) and Mg_3Bi_2 (purple line) in Eq. (3).

Table 1
Physical properties of the $Mg_3Sb_{2-x}Bi_x$ system.

Compound	Mg_3Sb_2 (x = 0)	$Mg_3Sb_{1.5}Bi_{0.5}$ (x = 0.5)	Mg_3SbBi (x = 1.0)	$Mg_3Sb_{0.5}Bi_{1.5}$ (x = 1.5)	Mg_3Bi_2 (x = 2)
Bulk modulus, B (GPa)	45.9	47.5	45.3	–	–
	36.4 [6]				38.4 [6]
	42 [33]				37 [33]
Shear modulus, G (GPa)	16.0	16.4	15.5	–	–
	15.7 [6]				13.4 [6]
	19 [33]				15 [33]
Poisson ratio, ν	0.34	0.34	0.35	–	–
	0.32 [33]				0.32 [33]
Molar volume, V_m (m^3mol^{-1})	7.86E-05	7.98E-05	8.09E-05	8.23E-05	8.35E-05
Debye temperature (K)	230 ± 2[a]	216 ± 4[a]	199 ± 2[a]	191 ± 1[a]	177 ± 2[a]
	228 ± 4[b]	218 ± 3[b]	201 ± 3[b]	–	–

[a] Debye temperature determined from low-temperature heat capacity; error estimated from the range of heat capacity values.
[b] Debye temperature determined from speed of sound; error estimated from the error in the speed of sound measurements (<2%).

$10^{-6}K^{-1}$). The temperature dependence of α_V, which is constant at high temperature but goes to zero at 0 K, can be neglected because the $B\alpha_V^2$ term is already relatively small and is multiplied by the absolute temperature (Eq. (2)), effectively suppressing the dilation contribution below 150 K. As T increases, however, the dilation term is necessary to account for the deviation of the measured C_p from C_v (compare dashed and solid lines in Fig. 2).

The success of using the physics-based model (Eq. (2)) to describe the low-temperature heat capacity (Fig. 2) provides validation for using the model to describe the heat capacity over the full temperature range (Fig. 3). Particularly, by demonstrating that the model correctly captures the magnitude and curvature of C_p leading up to 300 K means that extrapolation to higher temperatures is self-consistent with low-temperature measurements. Because the molar heat capacities of the entire compositional range ($0 \leq x \leq 2$) are similar at low temperatures (e.g. the spread in values is <5% of the mean at 220 K), the C_p model for Mg_3Sb_2 can be used as a good approximation for the entire system. For temperatures from 100 to 220 K, the model is within 1% of the average of the experimental values. Then, the error of the model can be estimated from the range of the 5 data sets as approximately ±3%. As can be seen in Fig. 3, measurements of high-temperature (>300 K) heat capacity in the $Mg_3Sb_{2-x}Bi_x$ system vary substantially in magnitude (≈20% at 400 K, see Fig. 3). This is likely the result of the sensitivity of measurement techniques (e.g. differential scanning calorimetry) to baseline corrections/calibration. Nonetheless, the high-temperature slopes of the measured C_p values (dC_p/dT) are qualitatively consistent with those predicted from the bulk modulus and thermal expansion. This supports the idea that measurements are prone to systemic errors that lead to differing absolute magnitudes between studies, whereas relative magnitudes (i.e. dC_p/dT) agree. Thus, the model is likely a better estimate of the magnitude of the high-temperature C_p because it is consistent with the low-temperature values and reproduces the linear slope observed in the high-temperature measurements.

In recognizing that the molar heat capacities of the $Mg_3Sb_{2-x}Bi_x$ system are similar (Fig. 3) and can be estimated by a simple model (Eq. (2)) over the full temperature range (grey line in Fig. 3), it is advantageous to make the model values of C_p accessible for engineering applications. Herein, a Maier–Kelly [32] polynomial expression was found to describe the model curve (normalized RMS error of 0.2%), and thus estimate the magnitude of experimental heat capacity ±3% for the range $200\ K \leq T \leq 800\ K$:

$$c_p\left[J\,g^{-1}K^{-1}\right] = \frac{3NR}{M_W}\left(1 + 1.3\times10^{-4}\,T - 4\times10^{3}\,T^{-2}\right), \qquad (4)$$

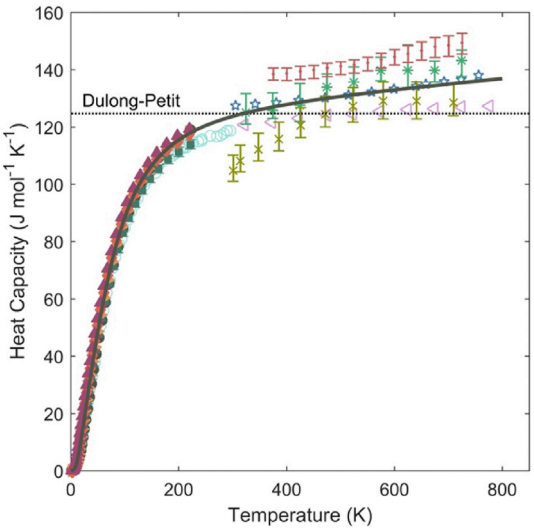

Fig. 3. A compilation of experimental heat capacity values for $Mg_3Sb_{2-x}Bi_x$ alloys over the full temperature range. The low-temperature values (<300 K) measured herein, x = 0 (grey circles), x = 0.5 (green squares), x = 1.0 (yellow triangles), x = 1.5 (orange diamonds), x = 2.0 (purple triangles), have magnitudes within ±3% of the Mg_3Sb_2 model curve (grey line) below 220 K. The experimental results of this study agree with the low-temperature values reported for Mg_3Sb_2 by Yoon [31] (open blue circles). The reported values at higher temperature (>300 K) are more scattered, with the measured values of this study (red dots) having the largest magnitude, but a slope in agreement with theory. The experimental values of Shuai et al. [17] (open blue stars) and Tamaki et al. [1] (green asterisk markers) agree best with both the magnitude and slope of the model curve. Bhardwaj and Misra [15] (open triangle markers) and Chen et al. [16] (gold X markers) report values somewhat lower in magnitude, but with similar slopes as the others. Note that the linear dilation term is responsible for increasing $C_p \approx 5\%$ above the Dulong–Petit value by 600 K.

where $3NR = 124.71$ J mol^{-1}K^{-1} in which $N = 5$ (number of atoms per formula unit) and R is the gas constant. M_W is the molecular weight of the formula unit being considered (in units of g mol^{-1}). By the Neumann–Kopp rule, this same expression is expected to hold when dopants/substitutions are introduced. In that case, an appropriate M_W should be used accordingly. Also note that Eq. (4) is written in a way that the unit dimensions may be easily changed. The dimensionless heat capacity $C_p/3nk_B$ is the polynomial term in parenthesis in Eq. (4).

The excellent agreement of Eq. (4) even for the full solid solution from Mg_3Sb_2 to Mg_3Bi_2 and its closeness to the Dulong–Petit value ($3NR/M_W$) suggests that Eq. (4) should be a good estimate even for doped (such as Te, Se, S, La n-type dopants [34,35] or Na, Li p-type dopants [36,37]) or alloyed (Ca, Zn, Cd, etc. up to ~30%) samples.

It should also be emphasized that the approach undertaken in this study to estimate C_p at high temperature may be readily applied to other material systems. Using a Maier–Kelly [32] polynomial to describe the Debye model for C_v (for $T > 0.5\theta_D$) and substituting in Eq. (2) gives

$$c_p\left[\mathrm{Jg^{-1}K^{-1}}\right] \approx \frac{3NR}{M_W}\left[1 + \frac{1}{10^4}\left(\frac{T}{\theta_D}\right) - \frac{1}{20}\left(\frac{T}{\theta_D}\right)^{-2}\right] + A\left(\frac{T}{\theta_D}\right), \quad (5)$$

where A is the dilation term in units of J g^{-1}K^{-1}, i.e. $A = BV_m\alpha_V^2\theta_D/M_W$. Alternatively, A can be found directly from the slope of high-temperature heat capacity measurements ($A \sim \theta_D{}^*dCp/dT$). The equivalence of Eq. (5) ($\theta_D = 282$ K) with Eq. (4) for $Mg_3(Sb,Bi)_2$ compounds provides compelling justification for the use of Eq. (5) to accurately estimate the heat capacity of other compounds at high temperature. In fact, Eq. (5) is typically more accurate than even experimental measurements not only for $Mg_3Sb_{2-x}Bi_x$ but also for other single-phase materials [18].

4. Conclusion

Including the first-order anharmonic correction to the harmonic phonon heat capacity provides an accurate description of experimental heat capacity of $Mg_3(Sb,Bi)_2$ up to 800 K. The self-consistency of the C_p model with both low- and high-temperature experimental results provides validation that it can be used to estimate the magnitude of high-temperature C_p where experimental results are scattered. The model is likely to be more accurate for a given new material than an individual measurement, considering the typical uncertainties of high-temperature heat capacity measurements. A simple polynomial expression is given for the suggested heat capacity values over the 200 K$\leq T \leq$ 800 K range that is expected to be accurate within ±3% for $Mg_3(Sb,Bi)_2$ solid solutions even when considering dopant and alloying additions. The high anharmonicity of $Mg_3(Sb,Bi)_2$ compounds leads to deviations of C_p from the Dulong–Petit limit at high temperatures. We recommend that the suggested values of C_p be used so that thermal conductivity is not appreciably underestimated and to improve accuracy of comparing results among different laboratories. The method is easily generalized to other materials.

Conflicts of interest

The authors declare no conflicts of interest, financial or otherwise.

Data availability

The raw data required to reproduce these findings are available from the corresponding authors upon request. The processed data required to reproduce these findings are available to download from the Materials Data Facility (https://doi.org/doi:10.18126/M22H1D).

Acknowledgments

The authors would like to thank Pawan Gogna for high-temperature heat capacity measurements and Samad Firdosy for high-temperature dilatometry measurements. The work in the Materials Science Division of Argonne National Laboratory (low-temperature heat capacity measurements) was supported by the U.S. Department of Energy, Office of Science, Basic Energy Sciences, Materials Sciences and Engineering Division, under contract No DE-AC02-06CH11357. Part of this work was performed at the California Institute of Technology/Jet Propulsion Laboratory under contract with the National Aeronautics and Space Administration. This work was supported by the NASA Science Missions Directorate under the Radioisotope Power Systems Program. S.A. and G.J.S. acknowledge support from the National Science Foundation (DMREF-1333335 and DMREF-1729487).

References

[1] H. Tamaki, et al., Adv. Mater. 28 (46) (2016) 10182.
[2] J. Shuai, et al., Mater. Today Phys. 1 (2017) 74.
[3] S. Ohno, et al., Joule 2 (1) (2018) 141.
[4] J. Zhang, et al., Nat. Commun. 8 (2017) 13901.
[5] K. Imasato, et al., Mater. Horiz. 5 (1) (2018) 59.
[6] W. Peng, G. Petretto, G.-M. Rignanese, G. Hautier, A. Zevalkink, An unlikely route to low lattice thermal conductivity: small atoms in a simple layered structure, Joule 2 (9) (2018) 1879–1893.
[7] T. Kanno, et al., Appl. Phys. Lett. 112 (3) (2018) 033903.

[8] J.J. Kuo, et al., Energy Environ. Sci. 11 (2) (2018) 429.
[9] J. Shuai, et al., Energy Environ. Sci. 10 (3) (2017) 799.
[10] K. Imasato, et al., Appl. Mater. 6 (1) (2018) 016106.
[11] J. Mao, et al., Proc. Natl. Acad. Sci. U. S. A. (2017) 201711725.
[12] J. Mao, et al., Mater. Today Phys. 3 (2017) 1.
[13] J. Mao, et al., ACS Energy Lett. 2 (10) (2017) 2245.
[14] W. Peng, et al., Inorg. Chem. Front. 5 (2018) 1744.
[15] A. Bhardwaj, D. Misra, RSC Adv. 4 (65) (2014) 34552.
[16] X. Chen, H. Wu, J. Cui, Y. Xiao, Y. Zhang, J. He, Y. Chen, J. Cao, W. Cai, S.J. Pennycook, Z. Liu, L.-D. Zhao, J. Sui, Extraordinary thermoelectric performance in n-type manganese doped Mg3Sb2 Zintl: High band degeneracy, tuned carrier scattering mechanism and hierarchical microstructure, Nano Energy 52 (2018) 246–255.
[17] J. Shuai, et al., Acta Mater. 93 (2015) 187.
[18] K.A. Borup, et al., Energy Environ. Sci. 8 (2) (2015) 423.
[19] H. Wang, et al., J. Electron. Mater. 42 (6) (2013) 1073.
[20] A. Zevalkink, et al., Appl. Phys. Rev. 5 (2) (2018) 021303.
[21] Y. Pei, et al., Energy Environ. Sci. 4 (6) (2011) 2085.
[22] R. Truell, et al., Ultrasonic Methods in Solid State Physics, Academic Press, 2013.
[23] O.L. Anderson, J. Phys. Chem. Solids 24 (7) (1963) 909.
[24] W. Kohn, et al., J. Phys. Chem. 100 (31) (1996) 12974.
[25] G. Kresse, J. Furthmüller, Phys. Rev. B 54 (16) (1996) 11169.
[26] J.P. Perdew, et al., Phys. Rev. Lett. 77 (18) (1996) 3865.
[27] A. Togo, I. Tanaka, Scripta Mater. 108 (2015) 1.
[28] J.W. Jaeken, S. Cottenier, Comput. Phys. Commun. 207 (2016) 445.
[29] M. Wood, et al., J. Mater. Chem. A 6 (20) (2018) 9437.
[30] O. Madelung, Semiconductors: Data Handbook, Springer Science & Business Media, 2012.
[31] H.,I. Yoon, Low Temperature Lattice Heat Capacities of Alloys: InPb, AuCd, Mg_3Sb_2. II. Effect of Ordering on Lattice Heat Capacity: $AuCu_3$, Ph.D. Thesis, Univ. of California, Berkeley, 1971.
[32] C.G. Maier, K. Kelley, J. Am. Chem. Soc. 54 (8) (1932) 3243.
[33] A. Jain, et al., Appl. Mater. 1 (1) (2013) 011002.
[34] J. Mater. Chem. A 6 (2018) 19941–19946.
[35] J. Zhang, et al., New insight on tuning electrical transport properties via chalcogen doping in n-type Mg_3Sb_2-based thermoelectric materials, Adv. Energy Mater. (2018), 1702776.
[36] Z. Ren, et al., Significantly enhanced thermoelectric properties of p-type Mg_3Sb_2 via co-doping of Na and Zn, Acta Materialia 143 (2018) 265–271.
[37] C. Chen, et al., Enhanced thermoelectric performance of p-type Mg_3Sb_2 by lithium doping and its tunability in an anionic framework, J. Mater. Sci. 53 (23) (2018) 16001–16009.